

1

2 **Comparing integrated water vapor sun photometer observations over the Arctic with**  
3 **ERA5 and MERRA-2 reanalyses.**

4 **J. C. Antuña-Marrero<sup>1,2</sup>, R. Román<sup>1</sup>, V. E. Cachorro<sup>1</sup>, D. Mateos<sup>1</sup>, C. Toledano<sup>1</sup>, A. Calle<sup>1</sup>,**  
5 **J. C. Antuña-Sánchez<sup>3,1</sup>, R. Gonzalez<sup>1</sup>, M. Antón<sup>4,5</sup>, J. Vaquero-Martínez<sup>6,5</sup> and Á. M. de**  
6 **Frutos Baraja<sup>1</sup>**

7 <sup>1</sup>Group of Atmospheric Optics (GOA-UVa), Universidad de Valladolid, 47011, Valladolid,  
8 Spain

9 <sup>2</sup>EphysLab, Departamento de Física Aplicada, Área de Física de la Tierra, Universidade de Vigo,  
10 Campus Sur, 32004 Ourense, España

11 <sup>3</sup>GRASP-SAS, Villeneuve d'Ascq, France

12 <sup>4</sup>Department of Physics, Universidad de Extremadura, 06006 Badajoz, Spain

13 <sup>5</sup>Instituto Universitario de Investigación del Agua, Cambio Climático y Sostenibilidad (IACYS),  
14 Universidad de Extremadura, 06006 Badajoz, Spain

15 <sup>6</sup>Departamento de Didáctica de las Ciencias Experimentales y las Matemáticas, Universidad de  
16 Extremadura, 10071 Cáceres, Spain

17  
18 Corresponding author: Juan Carlos Antuña-Marrero ([antuna@goa.uva.es](mailto:antuna@goa.uva.es))

19

20 **Key Points:**

21

- 22 Arctic IWV from reanalysis is moister than data from sun photometers. Daily means correlate more accurate but less precise than hourly
- 23 IWV differences between reanalyses and sun photometers are independent of sun photometer IWV vapor magnitudes and solar zenith angles
- 24 Sun photometer IWV observations may be used as a secondary standard for validating IWV from reanalyses in the Arctic

25

26

27

28 **Abstract**

29 Atmospheric water vapor, a greenhouse gas, is increasing in the Arctic. It is a scientific challenge  
30 to understand the causes for this increase and determine adaptation and mitigation actions to  
31 confront its climatic effects. During the last decades, spatial and temporal coverage of water  
32 vapor satellite observations increased notably, and reanalysis water vapor estimates have steadily  
33 improved. However, the scarce spatial and temporal coverage in the Arctic of integrated water  
34 vapor (IWV) surface-based observations, limits the representativeness of satellite observations  
35 and reanalysis estimate validations. Recently we validated sun photometer IWV (IWVsp)  
36 observations with IWV from radiosondes in the Arctic with good results. Here we compare the  
37 hourly and daily means of IWVsp from thirteen Arctic AERONET stations and the IWV from  
38 ERA-5 and MERRA-2 reanalyses. The comparison is conducted at hourly and daily time scales  
39 for individual stations, for two Arctic regions and for the whole Arctic. The comparison showed  
40 a moist bias of IWV from reanalyses with respect to IWVsp. For the individual stations the daily  
41 mean IWV from reanalyses increases in accuracy and correlation but decreases in the precision  
42 with respect to the hourly values. The individual station wise pattern shows slightly better  
43 accuracy and precision for ERA5 than for MERRA-2, also evident at the selected sub-regional  
44 scale. The differences of IWV from ERA5 and MERRA-2 and IWVsp show no dependence on  
45 IWVsp nor the solar zenith angle. This study corroborates that IWVsp may be used for  
46 validations of satellite IWV observations and IWV reanalyses products.

47 **Plain Language Summary**

48 Water vapor is increasing in the Arctic. Being a greenhouse gas, it is necessary to understand the  
49 causes for that increase. It will allow adaptation and mitigation actions for its climate effects.  
50 Progress in integrated water vapor (IWV) satellite observations and reanalyses estimates still do  
51 not match uncertainty levels from surface-based Arctic observations. However, the amount and  
52 geographical and temporal distributions of Arctic surface IWV observations is limited, limiting  
53 validation of spatial and temporal representativeness of IWV from satellite and reanalysis. We  
54 recently validated sun photometer IWV with radiosonde IWV, showing good agreement between  
55 those instruments. Here we report validating  $IWV_{ERA5}$  and  $IWV_{MERRA-2}$  reanalyses with sun  
56 photometer IWV. Hourly and daily mean IWV values from reanalyses were compared with sun  
57 photometer IWV for individual stations, two Arctic subregions, and the entire Arctic. The results  
58 showed that the IWV reanalyses overestimates sun photometer IWV, so called “moist bias”.  
59  $IWV_{ERA5}$  agrees better with sun photometer IWV than  $IWV_{MERRA-2}$  at all spatial scales. The  
60 differences between sun photometer IWV and IWV from reanalyses do not depend on the IWV  
61 amount, neither they have a diurnal cycle. The sun photometer IWV observations can serve as a  
62 secondary standard to validate the IWV reanalysis.

63 **1 Introduction**

64 Water vapor is associated with several important hydrological cycle processes in the  
65 Arctic. It is the source for the formation of clouds and fog but also has notable effects in the  
66 energy budget resulting from condensation-evaporation and radiative transfer processes (Vihma  
67 et al., 2016). Also, it plays an important role in the amplification of climate warming, caused by  
68 the Arctic hydrological cycle intensification resulting in the surface temperature increase (Box et  
69 al., 2019). However, it is particularly difficult to assess Arctic water vapor magnitude,  
70 geographical distribution and seasonal patterns because of two reasons. The First, its high spatial

71 and temporal variability, exemplified by the changes in atmospheric water vapor reaching 100%  
72 within a few hours under atmospheric river events (Crewell et al., 2021). Second, the lack of  
73 reliable water vapor observations due to the limited number of surface stations (Vihma et al.,  
74 2016). To cope with the last issue, some networks like AERONET (Aerosol RObotic NETwork;  
75 Holben et al., 1998) provide IWV than can be used as an independent source for validation. The  
76 lack of IWV observations spread widely throughout the Arctic means that current research on the  
77 Arctic's global hydrological budget heavily relies on atmospheric reanalyses data (e.g., Dufour et  
78 al. 2016; Vihma et al. 2016). Reanalysis consists of the assimilation of ground based and remote  
79 sensing observations in a consistent manner with model physics, resulting in long-term gridded  
80 datasets with physical interpolation into data-missing regions (Thorne and Vose 2010; Parker,  
81 2016). The products from reanalysis must be compared with real observations to establish their  
82 uncertainty and applicability. In this sense, an appreciable number of comparisons of reanalysis  
83 IWV products with ground based and satellite observations have been already reported  
84 extensively for the earlier generations of reanalyses (Schröder et al., 2016; 2018; 2019), although  
85 few cover the Arctic region (ex. Negusini et al., 2021). Among those comparisons, the Global  
86 Energy and Water cycle Exchanges (GEWEX) Water Vapor Assessment reported a general  
87 disagreement in IWV trend estimates for the global ice-free ocean within 60° N/S, from eleven  
88 global IWV datasets, including six reanalyses, with MERRA-2 among them, and five IWV  
89 satellite products. The trends in IWV are in the range from  $-1.51 \pm 0.17 \text{ kg m}^{-2} \text{ decade}^{-1}$  to  $1.22 \pm$   
90  $0.16 \text{ kg m}^{-2} \text{ decade}^{-1}$ . Break points on global and regional scales are also present (Schröder et al.,  
91 2017).

92 Comparisons of the IWV from the last generation of reanalyses, in particular European  
93 Centre for Medium-Range Weather Forecasts (ECMWF) 5th Re-Analysis (ERA5) and the  
94 NASA Global Modeling and Assimilation Office (GMAO) Modern-Era Retrospective Analysis  
95 for Research and Applications, Version 2 (MERRA-2) with IWV from ground-based instruments  
96 have been recently reported for several regions and worldwide (Schröder et al., 2016; 2018;  
97 2019). However, those reports do not include comparisons of IWV from ERA5 and/or MERRA-  
98 2 with AERONET IWV product focusing on the Arctic.

99 We recently reported the comparison of IWV observations from radiosondes and IWV  
100 from AERONET sun photometers (IWVsp) at ten sites located across the Arctic (Antuña-  
101 Marrero et al., 2022). At those sites, it was identified the predominant dry bias of AERONET  
102 IWV observations with respect to radiosondes, already reported at midlatitudes and tropical sites.  
103 At eight out of ten stations, using onsite sounding systems with state of the art humidity sensors  
104 and retrieval algorithms, precision and accuracy obtained were below 8% and 2%, respectively  
105 (Antuña-Marrero et al., 2022). One of the main conclusions of the study was the capability of  
106 AERONET water vapor observations in the Arctic for research, considering the robust  
107 quantification of its dry bias established in the cited study. Based on the former conclusion, and  
108 the fact that AERONET uses standard instruments and a centralized-standard processing  
109 algorithm, we also concluded that the AERONET water vapor observations in the Arctic could  
110 be used as a secondary standard to re-calibrate or homogenize other integrated water vapor  
111 datasets in the Arctic (Antuña-Marrero et al., 2022). The present study, based on the two above-  
112 mentioned conclusions, and taking advantage of the geographical regular grid and high

113 resolution of the ERA5 and MERRA-2 reanalyses, is aimed at comparing the water vapor from  
114 both reanalyses with the available AERONET water vapor observations.

115 We report the validation of IWV from ERA5 and MERRA-2 with the IWVsp product  
116 from 13 AERONET sites in the Arctic. In section 2, we describe IWVsp datasets from  
117 AERONET sun photometers and the reanalyses ERA5 and MERA-2, as well as the spatio-  
118 temporal coincidence criteria applied. We also show and discuss in that section the correction of  
119 the reanalyses IWV values by the differences in elevation between each AERONET site and the  
120 elevation of the 4 surrounding grid points for each reanalysis. The statistics used for the  
121 comparison are also described. Section 3 shows the results and discussion. Finally, the  
122 conclusions are provided in section 4.

## 123 **2 Materials and Methods**

### 124 **2.1 Sun photometer IWV observations**

125 The main dataset of this work consists of IWVsp observations from AERONET version 3  
126 level 2.0 daytime products (Giles et al., 2019; AERONET, 2023), recorded by sun photometers  
127 located within the Arctic circle. A detailed explanation of the AERONET version 2 basic  
128 processing algorithm of the IWVsp observations is available in Pérez-Ramírez et al., (2014).  
129 Improvements introduced in version 3 include: temperature correction for all spectral channels in  
130 all AERONET instruments using the sensor head temperature; and the use of solar aureole  
131 radiance for cirrus cloud-screening (Giles et al., 2019).

132 The lack of sunlight during the polar night limits the availability of IWVsp AERONET  
133 data in winter. However, the scarcity of spatially and temporally distributed IWV observations in  
134 the Arctic makes the IWVsp AERONET dataset a unique source of information to complement  
135 and validate other available IWV datasets in the region. The uncertainty on this AERONET  
136 IWVsp product is typically less than 12% (Holben et al., 1998).

137 The AERONET IWVsp values have been hourly averaged in the interval of  $\pm 30$  minutes  
138 around each hour using all the available instantaneous observations in each interval. Then, daily  
139 IWVsp averages have been calculated averaging these hourly IWVsp data for each available day.

140 Table 1 lists the 20 AERONET stations that are available in the Arctic, providing information  
141 about its geographical location, number of available instantaneous observations, hourly and daily  
142 calculated IWVsp values and the observation period. The representativeness of the 20 datasets  
143 was evaluated considering its spatial and temporal coverage and the station mean quantity of  
144 hourly observations.

145 The first step was to exclude the stations with less than 2 years of data. The excluded stations  
146 were Matorova FMI, Abisko, Ny Ålesund, and North\_Pole. Then we identified the stations  
147 located less than  $0.25^\circ$  apart both in latitude and longitude and with altitude differences lower  
148 than 100 m. Barrow and NEON BARR were found to satisfy these criteria and the shorter  
149 duration dataset NEON BARR was discarded. Finally, we decided to exclude the stations of  
150 NEON TOOL and Longyearbyen because they have less than 20% of the average number of  
151 hourly observations. The reason to exclude the stations with less than 2 years of data or less than  
152 20% of the station average number of hourly observations (i.e., 1500 observations) was a  
153 reasonable size of the observation samples at each of the stations to warrant robust statistics. In

154 the case of the stations located less than  $0.25^{\circ}$  apart and a difference in altitude lower than 100  
155 m, the goal was to eliminate duplicated observations at the same geographical location. The 7  
156 discarded stations are highlighted on Table 1 by a grayish background.

157 A number and an ID have been assigned to the 13 selected stations on Table 1. The total  
158 number of available sun photometer IWV data is also shown in Table 1 for instantaneous  
159 observations (601,029), hourly mean values (98,185), and daily mean values (12,158) for the 13  
160 selected stations. Figure 1 shows the geographical distribution, identified by the red stars, of the  
161 13 selected stations in the Arctic. Blue stars and names identify Greenland and European Arctic  
162 (GEA) stations while Russia, Alaska, and Canadian Arctic (RACA) stations are identified by  
163 brown diamonds and names. The encircled red star represents the very close OPAL and PEARL  
164 stations in North Canada.

## 165 2.2 Hourly coincident IWV values from ERA5 and MERRA-2 Reanalyses

166 Regarding reanalysis data, we have used the IWV hourly data from ERA5 and MERRA-2  
167 described by Hersbach et al. (2020) and Gelaro et al. (2017), respectively. IWV data from ERA5  
168 ( $\text{IWV}_{\text{ERA5}}$ ) and MERRA-2 ( $\text{IWV}_{\text{MERRA-2}}$ ) are available for each hour. ERA5 is a new ECMWF  
169 global atmospheric reanalysis model replacing ERA-Interim (stopped being produced on August  
170 2019). It provides hourly estimates of atmospheric variables at a spatial resolution of  $0.25^{\circ} \times$   
171  $0.25^{\circ}$  (Hersbach et al., 2020). Similarly, MERRA-2 is a new GMAO atmospheric reanalysis  
172 model replacing the original MERRA, discontinued in February 2016. The hourly atmospheric  
173 variable products have a coarser spatial resolution of  $0.5^{\circ} \times 0.625^{\circ}$  (Gelaro et al., 2017). Most of  
174 the global temperature and moisture products in ERA5 and MERRA-2 are determined from the  
175 direct assimilation of satellite radiances. Those radiances are currently the main source of  
176 information to produce the water vapor profiles and the integrated water vapor in ERA5  
177 (ECMWF, 2016; Hersbach et al. 2020) and in MERRA-2 (McCarty et al., 2016; Gelaro et al.,  
178 2017).

179 A preliminary spatial and temporal coincidence criterion to select the IWV values from  
180 ERA5 and MERRA-2 consisted in selecting the four grid points around the location of each  
181 AERONET station with the same dates of the IWV<sub>SP</sub>, producing a first reanalysis dataset. Then,  
182 a subset of the former dataset was generated retaining only the four grid points coincident only  
183 with the hours in which at least one IWV<sub>SP</sub> observation is available. Both datasets were subject  
184 to bilinear interpolation and correction procedures described below.

## 185 2.3 Correcting reanalysis IWV values

186 For the AERONET-reanalysis comparison, the hourly IWV values from ERA5 and  
187 MERRA-2 have been corrected by the difference in altitudes of the surrounding reanalysis grid  
188 points and the altitude of the corresponding AERONET station. For each of the reanalysis, both  
189 the IWV magnitude and the altitudes at the 4 grid points around the AERONET station location  
190 were bi-linearly interpolated to the AERONET station geographical coordinates. The bilinear  
191 interpolated altitudes ( $H_{\text{Rean}}$ ) were used to calculate  $\Delta H = H_{\text{Rean}} - H_{\text{SP}}$  at each site, where the  
192 term  $H_{\text{SP}}$  is the altitude of the AERONET station and  $H_{\text{Rean}}$  is the mean of the altitudes of the  
193 four surrounding Reanalysis points. The bi-linearly interpolated  $\text{IWV}_{\text{Rean}}$  and the corresponding  
194  $\Delta H$  were then used to calculate the corrected IWV values from ERA5 ( $\text{IWV}_{\text{ERA5}}$ ) and MERRA-2

195 (IWV<sub>MERRA-2</sub>) using the next equation (1) for both reanalyses (Leckner, 1978; Wang, Y. et al.,  
196 2017; Wang, S. et al, 2020; Zhu et al., 2021):

197 
$$IWV_{Rean} = IWV_{Rean} \exp \left( \frac{C_2 \Delta H}{1,000} \right) \quad (1)$$

198 where the value C<sub>2</sub> is equal to 0.439 m<sup>-1</sup> (Leckner, 1978), the exponential term is the  
199 altitude correction coefficient, and the subscript *Rean* refers to both reanalyses.

200 The altitudes of the AERONET sites and the coincident bilinearly interpolated altitudes  
201  $H_{ERA}$  and  $H_{MERR}$  are shown on the top panel of Figure 2, where the station numbers are the ones  
202 listed on Table 1. The IWV correction coefficients, in the bottom panel of Figure 2, show that  
203 the maximum values of the altitude correction factors (1.105 and 1.144) for both ERA5 and  
204 MERRA-2 are found at Ny Ålesund AWI, and the minimum at PEARL station (0.802 and  
205 0.828). These are the sites with higher positive and negative altitude differences respectively.

206 

## 2.4 Processing

207 The comparison has been conducted for individual stations, for two regions and for the  
208 whole Arctic. The hourly time scale was selected because it is the reanalysis temporal resolution.  
209 The daily time scale was included because it is an intermediate scale between the hourly  
210 reanalysis' resolution and the typical residence time (~1 week) for the water vapor in the Arctic  
211 (Vihma et al., 2016). Daily means were calculated using the spatial and temporal coincident  
212 values of IWV<sub>sp</sub>, IWV<sub>ERA5</sub> and IWV<sub>MERRA-2</sub> for each individual station. Two already defined  
213 geographical regions have been considered also in this study. They were defined for the  
214 comparison of the IWV from sun photometers and radiosondes. The sun photometer only diurnal  
215 observations were required to match the respective maximum amounts of the available diurnal  
216 radio sounding observations 12:00 Local Time (LT) at meridians 0° and 180°. As mentioned, the  
217 regions are Greenland and European Arctic (GEA), ± 90° around the meridian 0°; and Russia,  
218 Alaska, and Canadian Arctic (RACA), ± 90° around the meridian 180°. (Antuña-Marrero et al.,  
219 2022). These two geographical regions also match the regions of the Atlantic and Pacific Arctic,  
220 associated to the respective sub-Arctic oceans (Mauritzen et al., 2013). A total of four stations  
221 are in the RACA region: ARM Oliktok AK, Barrow, Tiksi and Resolute Bay, while the other  
222 nine stations fall inside the GEA.

223 

### 2.4.1 Selected Statistics

224 Two main statistical indicators were selected for comparing IWV from reanalysis and  
225 photometer: 1) the Mean Bias Error (MBE), which defines the mean of  $\Delta IWV$  ( $IWV_{Rean} -$   
226  $IWV_{sp}$ ) and quantifies the accuracy on  $IWV_{Rean}$ , and 2) the standard deviation (STD) of the

227 differences between  $IWV_{Rean}$  and IWVsp, representing the precision of  $IWV_{Rean}$ . Both  
228 statistics are defined in equations (2) and (3), respectively:

229 
$$MBE = \frac{1}{N} \sum_{j=1}^N [\Delta IWV_j] \quad (2)$$

230 
$$STD = \sqrt{\frac{1}{N} \sum_{j=1}^N [\Delta IWV_j - MBE]^2} \quad (3)$$

231 where  $\Delta IWV_j$  is the difference between  $IWV_{Rean}$  and  $IWV_{sp}$  values, and N is the  
232 number of pairs of coincident AERONET and reanalysis data. The relative magnitude (in %) of  
233 STD (rSTD) and MBE (rMBE) have been determined dividing each term by the mean value of  
234 the N observations of IWVsp. In addition, the Pearson linear correlation coefficient (R) and the  
235 slope of the linear regression fit between IWVsp and  $IWV_{Rean}$  have been calculated.

### 236 3 Results and discussion

#### 237 3.1 Comparison for the individual stations

##### 238 3.1.1 Hourly means

239 Table 2 shows the statistics and linear fits from the comparisons between hourly  $IWV_{ERA}$   
240 vs IWVsp (hereinafter ERA5) and hourly  $IWV_{MERRA-2}$  vs IWVsp (hereinafter MERRA-2) for  
241 each one of the 13 stations. For all the stations, the magnitudes of STD (rSTD), show slightly  
242 higher values, in the order of 0.01 cm (1 to 7 %), for MERRA-2 than for ERA5. It reveals  
243 slightly better precision for  $IWV_{ERA5}$  than for  $IWV_{MERRA-2}$  values. In the case of MBE (rMBE), it  
244 is in general slightly higher for  $IWV_{MERRA-2}$  than for  $IWV_{ERA5}$ , showing values between 0.1 cm  
245 and 0.01 cm (3 and 14 %); this points to better accuracy for  $IWV_{ERA5}$  compared to  $IWV_{MERRA-2}$   
246 dataset. In the case of Hornsund, MBE (rMBE) shows slightly higher accuracy from  $IWV_{MERRA-2}$   
247 than for  $IWV_{ERA5}$ .

248 The statistics associated to the linear fit show that the slopes for ERA5 are slightly lower  
249 (with differences in the order of 0.1 to 0.01) than for MERRA-2 at 11 of the stations. In the other  
250 2 stations, Ny Ålesund AWI and Hornsund, the slopes for ERA5 are slightly higher (differences  
251 in the order of 0.01) than for MERRA-2. The values of R at 9 stations are slightly higher (in the  
252 order of  $10^{-2}$ ) for ERA5 than for MERRA-2 with no change in the rest. In general, the results  
253 reveal better accuracy and precision for hourly IWV values from ERA5 than from MERRA-2.

254 For ERA5 (Table 2) the STD values range between 0.25 cm (Barrow) and 0.08 cm  
255 (Thule) while rSTD ranges between 11.0% (Ittoqqortoormiit) and 29.7% (PEARL). The absolute  
256 MBE values range between 0.34 and 0.01 cm at Barrow and Kangerlussuaq, respectively, and for  
257 rMBE the absolute values range between 50.9 and 0.06 % at PEARL and Kangerlussuaq. For  
258 MERRA-2 the range of STD values is between 0.28 and 0.09 cm at Barrow and Thule  
259 respectively while for rSTD it ranges from 37.4 at PEARL down to 12.9 % at Ittoqqortoormiit.  
260 Absolute MBE values range from 0.36 to 0.02 cm at Barrow and Ittoqqortoormiit, respectively,  
261 and for rMBE absolute values it is 60.3 to 2.7 % at PEARL and Ittoqqortoormiit. Regarding the  
262 linear fits for ERA5 the slopes are in the range 1.43 and 0.87 at PEARL and Thule with 12 of the  
263 stations having slopes between 0.8 and 1.2. For MERRA-2 the range is between 1.55 at PEARL

264 and 0.89 at Thule, broader than the former. For ERA5, 7 stations have slopes in the range of  $1.0 \pm 0.1$ , while for MERRA-2 only 4 are in the cited range.

266 The results described above show a clear pattern for both ERA5 and MERRA-2: Barrow  
267 has the lower absolute precision and accuracy while PEARL shows the lower relative precision  
268 and accuracy. Conversely, for the higher accuracies and precisions the only common pattern for  
269 ERA5 and MERRA-2 is that Thule has the higher absolute precision for both of them. Then, for  
270 ERA5, Kangerlussuaq shows the higher absolute and relative accuracies and Ittoqqortoormiit the  
271 higher relative precision. Meanwhile, for MERRA-2, Ittoqqortoormiit has higher relative  
272 precision and the higher absolute and relative accuracies.

273 When R is compared among stations, for ERA5 its values are in the range 0.99 to 0.95 at  
274 Ny Ålesund AWI and Tiksi respectively. For MERRA-2 the range is 0.98 (Ny Ålesund AWI and  
275 Sodankyla) to 0.94 (Resolute Bay). The former results support the previous characterization,  
276 showing that, in general at station level, the  $IWV_{ERA5}$  values match slightly better the observed  
277  $IWV_{sp}$  than the  $IWV_{MERRA-2}$ .

### 278 3.1.2 Daily means

279 Table 3 is analogous to Table 2, but for the daily means of  $IWV_{sp}$ ,  $IWV_{ERA5}$  and  
280  $IWV_{MERRA-2}$ . For all the stations the comparison of the magnitudes of STD, rSTD, absolute MBE  
281 and absolute rMBE values between daily means of ERA5 and MERRA-2 show the same pattern  
282 than for hourly values in Table 2: slightly higher precision in  $IWV_{ERA5}$  than in  $IWV_{MERRA-2}$  for  
283 all the stations and slightly higher accuracy also in 11 stations for  $IWV_{ERA5}$  than in  $IWV_{MERRA-2}$ ,  
284 but higher for  $IWV_{MERRA-2}$  at Thule and Hornsund. Only 5 slopes from the linear fits for both  
285 ERA5 and MERRA-2 are in the range of  $1.0 \pm 0.1$ . In the case of R, as found for the hourly  
286  $IWV_{ERA5}$  and  $IWV_{MERRA-2}$ , its magnitudes slightly decrease at 7 stations in the fits of MERRA-2  
287 with respect to the fits of ERA5, with the other 6 showing no change.

288 The comparison of the hourly and daily statistics on Tables 2 and 3 reveals a slight  
289 decrease in the magnitudes of STD and rSTD between hourly and daily means of ERA5 and also  
290 between hourly and daily means of MERRA-2, implying also a slight increase of the precision.  
291 For the absolute values of MBE (rMBE) the stations show a slight increase at 6 stations in the  
292 order of 0.01cm (1 %) and lower than those at the remaining 7 stations.

293 For the linear fit results, when the hourly and daily statistics reported in Tables 2 and 3  
294 are compared, the number of stations with slopes for ERA5 in the range of  $1.0 \pm 0.1$  decreases  
295 from 7 for hourly values to 5 for the daily means. For MERRA-2, up to 5 stations remain in that  
296 range both for hourly and daily values. In the case of R, both for ERA5 and MERRA-2 the daily  
297 mean R values at all the stations are higher in the order of 0.01 than the corresponding hourly  
298 values. Overall, there is almost no difference between hourly and daily statistics.

### 299 3.2 Comparison for GEA and RACA regions and for all the stations

300 The statistics of the comparison considering the data in the GEA and RACA regions and  
301 all the stations together, are provided in Table 4 for hourly and daily means. This table shows,  
302 for all regions and for both ERA5 and MERRA-2, a slight increase in the absolute and relative  
303 precision (decrease in STD and rSTD in the orders of  $10^{-2}$  cm and 2 to 3 % respectively) in the

304 daily means of ERA5 and MERRA-2 with respect to the hourly values. For MBE and rMBE a  
305 similar pattern is present between hourly and daily mean values. Both the slopes and R also have  
306 a similar pattern.

307 When comparing ERA5 with MERRA-2, it could be noted an increase of 0.05 cm or  
308 lower (6% or lower) for STD (rSTD), and about 0.06 cm or lower (7% or lower) for MBE  
309 (rMBE). The slopes increase also by 0.1 or lower and R decreases 0.02 or less. There are no  
310 significant differences between GEA and RACA regions.

311 We have also compared the accuracy for all stations of the hourly  $IWV_{ERA}$  and  
312  $IWV_{MERRA-2}$  with the accuracy reported for the comparison between the  $IWV_{sp}$  and  $IWV$  from  
313 radiosondes (Antuña-Marrero et al. 2022). The accuracies (MBE) for all the stations of the  
314 hourly  $IWV_{ERA5}$  and  $IWV_{MERRA-2}$  (All Hr) in Table 4 are 0.10 and 0.15 cm respectively. Those  
315 values are about three times higher than the accuracy of -0.02 cm reported for the  $IWV_{sp}$  for the  
316 set of 10 stations (All sites<sup>(1)</sup>) in comparison with radiosondes (see Table 3 of Antuña-Marrero et  
317 al., 2022). In addition to the lower accuracy in the case of the reanalyses, they demonstrate a  
318 moist/dry bias with respect to the  $IWV_{sp}$  in the order of  $10^{-1}$  cm. Moreover, the  $IWV_{sp}$   
319 demonstrate a moist/dry bias with respect to the  $IWV$  from radiosondes in the order of  $10^{-2}$  cm,  
320 an order of magnitude lower than the moist bias of the reanalyses with respect to the  $IWV_{sp}$ . As  
321 a conclusion,  $IWV_{ERA5}$  and  $IWV_{MERRA-2}$  have also a moist bias with respect to the  $IWV$  from  
322 radiosondes.

323 Considering now the precision for the same two sets of stations, the comparison with  
324  $IWV_{ERA}$  and  $IWV_{MERRA}$  shows (Table 4) the relative precisions of 24.9 and 29.5 % respectively.  
325 In the case of the comparison with the  $IWV$  from radiosondes (Table 3 of Antuña-Marrero et al.,  
326 2022) the precision was 8 %. Then the precision of reanalysis data with respect to the  $IWV$  from  
327 radiosondes could be estimated as 15 % and 20 % for  $IWV_{ERA5}$  and  $IWV_{MERRA-2}$ , respectively. A  
328 more conservative estimate, considering the 12 % estimated precision for AERONET  $IWV$   
329 observations (Holben et al., 1998), the uncertainty in both reanalyses is, respectively, about 13 %  
330 and 18 %.

331 Figure 3 provides a visual perspective of the former results, evidencing the very slight  
332 differences between the linear fits for  $IWV_{ERA5}$  and  $IWV_{MERRA-2}$  with  $IWV_{sp}$  for all the stations  
333 together. The differences in the slopes and R between ERA5 hourly and daily means (left two  
334 panels) are 0.03 and 0.02 while for MERRA-2 (right two panels) are 0.03 and 0.01, showing no  
335 major differences. If we compare hourly ERA5 and MERRA-2 (top two panels) the slope  
336 increased for MERRA-2 by 0.08 but R is unchanged. In the case of daily means ERA5 and  
337 MERRA-2 (bottom two panels) the slope increased for MERRA-2 also 0.08 but R decreased  
338 0.01.

339 3.3 Hourly  $\Delta IWV_{ERA5}$  and  $\Delta IWV_{MERRA-2}$  dependence on the  $IWV_{sp}$  and the solar zenith  
340 angle

341 The possible dependence of the hourly  $\Delta IWV_{ERA5}$  and  $\Delta IWV_{MERRA-2}$  on the  $IWV_{sp}$   
342 observations and the solar zenith angle (SZA) was evaluated. To that end, the linear fits between  
343 hourly  $\Delta IWV_{ERA5}$  and  $\Delta IWV_{MERRA-2}$  with the  $IWV_{sp}$  values and with the SZA of the  
344 observations were calculated. Table 5 reports the values of R from the linear fits of the hourly

345  $\Delta\text{IWV}_{\text{ERA5}}$  and  $\Delta\text{IWV}_{\text{MERRA-2}}$  with IWVsp and SZA for each of the stations. The magnitudes of  
346 R show higher values for MERRA-2 than for ERA5, but the higher R values for both are lower  
347 than 0.8 showing low correlation. R values for the linear fits with IWVsp higher than 0.5  
348 (shadowed in gray) occurs at 4 stations (Sodankyla, Andenes, Barrow and PEARL) both for  
349 ERA5 and MERRA-2, and at OPAL for MERRA-2. In the rest of the cases, for R lower than 0.5  
350 we also find 3 negative values of R for ERA5 and 2 for MERRA-2. It is relevant the fact that the  
351 highest values of R occur at PEARL (0.76 for ERA5 and 0.77 for MERRA-2), the same location  
352 that reported the highest values of rSTD and rMBE in tables 2 and 3, i.e. the lowest relative  
353 precision and accuracy among all the stations. In a similar way Barrow, having (Table 5) the  
354 second highest R value for ERA5 and the third higher for MERRA-2, has the highest STD and  
355 MBE values in tables 2 and 3, associated with the lowest precision and accuracy for all the  
356 stations. The former results support the hypothesis that, at both stations, the magnitude of the  
357 errors increase as the IWVsp increases.

358 Figure 4 shows the scatter plots of  $\Delta\text{IWV}_{\text{ERA5}}$  vs. IWVsp (top left) panel and  
359  $\Delta\text{IWV}_{\text{MERRA-2}}$  vs. IWVsp (top right panel) for all the stations together. Both for  $\Delta\text{IWV}_{\text{ERA5}}$  and  
360  $\Delta\text{IWV}_{\text{MERRA-2}}$  the trend shows that their magnitudes increase as IWVsp increases. R values are  
361 low for both reanalyses, with higher values for MERRA-2, similar as it was found for the  
362 individual stations. R is approximately in the range 0.3 to 0.4. Both scatter plots illustrate that  
363  $\Delta\text{IWV}_{\text{ERA5}}$  and  $\Delta\text{IWV}_{\text{MERRA-2}}$  range from 0 to 1.5 cm, displaying an extensive cloud of data. The  
364 data scatter is lowest for the extreme values of IWVsp (0 cm and 3 cm).

365 The R values of the linear fits between the hourly  $\Delta\text{IWV}$  from both reanalyses and SZA  
366 are also shown in Table 5. In this case the maximum R value is 0.2, representative of no  
367 correlation between the variables at the station level. In the bottom panel of Figure 4 the scatter  
368 plots of the hourly  $\Delta\text{IWV}$  from both reanalyses and SZA, shows a similar data scatter range (0  
369 cm to 1.5 cm) than for the dependence on IWVsp; however, the data show no dependence at all  
370 of  $\Delta\text{IWV}_{\text{ERA5}}$  and  $\Delta\text{IWV}_{\text{MERRA-2}}$  with respect to SZA. Moreover, the R of the fits with SZA, for  
371 all the stations, is in the order of  $10^{-2}$  (Figure 4), i.e negligible compared to the R for the fits vs.  
372 IWVsp. The main results discussed in this section show that the main sources of the  $\Delta\text{IWV}_{\text{ERA5}}$   
373 and  $\Delta\text{IWV}_{\text{MERRA-2}}$  are associated to the respective reanalyses.

### 374 3.4. Discussion

375 The results of the comparisons, shown on Tables 2, 3 and 4, of hourly and daily  $\text{IWV}_{\text{ERA5}}$   
376 and  $\text{IWV}_{\text{MERRA-2}}$  vs IWVsp at the stations, the GEA and RACA regions and for all the stations  
377 together show, in general, that IWV values from ERA5 perform better than MERRA-2 both in  
378 precision and accuracy. The main reason has already been identified to be the ERA5 higher  
379 spatial resolution (Huang et al., 2021; Yuan et al., 2023). Because the AERONET stations do not  
380 exactly match the reanalyses grid points, the spatial adjustment is applied using the nearby grid  
381 points. An additional adjustment considering the topography is applied, both described in section  
382 2.3. The larger spatial separation of the reanalysis at the nearby grid points increases the  
383 uncertainty in the spatial adjustments used for IWV match-up. In addition, the coarser

384 topography mask of the reanalyses increases the uncertainties of the topographic adjustment,  
385 more enhanced at highly variable topography.

386 The comparison also shows a moist bias of the IWV from both reanalyses with respect to  
387 the IWV<sub>sp</sub>. This feature has already been documented and explained. In the Arctic, reanalyses  
388 (including ERA5 and MERRA-2) have a poor representation of the vertical profiles of  
389 temperature and specific humidity inversions at 875 hPa, causing warm and dry biases at this  
390 level. There are also collocated specific and relative humidity inversions at 750 and 600 hPa.  
391 ERA5 and MERRA-2 simulated the inversion at 750 hPa. However, the one at 600 hPa is  
392 missing in the reanalyses. Then the reanalyses are too moist above 800 hPa, with MERRA-2  
393 moister than ERA5 (Graham et al., 2019).

394 The comparison of the hourly ERA5 and MERRA-2 vs IWV<sub>sp</sub> for all the 13 stations  
395 (Table 4), show STD (rSTD) of 0.21 cm (25 %) for ERA5 and 0.24 cm (30 %) for MERRA-2.  
396 However, for the 10 Arctic stations used in the comparison between IWV<sub>sp</sub> and IWV from  
397 radiosondes reported in Table 3 from Antuña-Marrero et al. (2022), the same statistic indicators  
398 had a value of 0.09 cm (10.4 %). This means that the IWV values from both reanalyses in the  
399 Arctic are less precise by an order of magnitude in the absolute IWV. Their precisions are also  
400 between 2 and 3 times lower for the relative values with respect to the IWV from radiosondes.  
401 The absolute magnitudes of MBE (rMBE) for all the stations in the current study are 0.10 cm (12  
402 %) and 0.15 cm (18 %) for ERA5 and MERRA-2, respectively. In contrast with the cited study,  
403 they are 0.01 cm (1 %) for the comparison of IWV<sub>sp</sub> and the IWV from radiosondes, thus also  
404 an order of magnitude higher in the current study. It means that the accuracy (absolute and  
405 relative) is lower for both reanalyses by an order of magnitude with respect to the IWV from  
406 radiosondes. Regarding the linear fit, the magnitude of the R value in the present study is 0.95  
407 and in the cited comparison of IWV<sub>sp</sub> with IWV from radiosondes, it was 0.99. The analysis  
408 above and the cited scarcity and inhomogeneity of IWV observations suggest that AERONET  
409 sun photometer IWV observations could be used as a secondary standard in the Arctic (WMO,  
410 2021). AERONET is characterized by its standardized instrumentation, centralized processing,  
411 quality control, and calibration services. These are unique features among instruments  
412 performing IWV observations in the Arctic. We found no reports of comparison between IWV<sub>sp</sub>  
413 and IWV from ERA5 and MERRA-2 reanalyses focused on the Arctic. However, there are some  
414 comparisons between IWV observations from Global Positioning System (GPS) and ERA5 and  
415 MERRA-2 reanalyses using broad geographical regions and including few Arctic sites. The GPS  
416 technique has proven to be a reliable method for retrieving atmospheric water vapor (e.g.,  
417 Vaquero-Martinez and Antón, 2021). A recent study has compared IWV time series from several  
418 reanalyses vs. GPS-derived IWV (IWV<sub>GPS</sub>) from 108 GPS stations for more than two decades  
419 (1994-2018) over Europe (Yuan et al., 2021). It includes 4 stations from the Arctic but does not  
420 provide quantitative information on them. For the entire region, it revealed IWV from ERA5 was  
421 the best in matching the diurnal variability in IWV<sub>GPS</sub> observations, followed by MERRA-2 as  
422 the second best. In addition, the comparison of both ERA5 and MERRA-2 with GPS IWV daily  
423 means for the entire region, STD values of 0.05cm to 0.16cm and 0.07cm to 0.23cm,  
424 respectively, are reported. For the linear fits, mean R values of 0.996 and 0.991 are found.  
425 Comparing with the present study of daily mean values (Table 3), the STD range from 0.07cm to  
426 0.22cm for ERA5 and from 0.08cm to 0.25cm for MERRA-2, quite similar except in the upper  
427 values for ERA5, which are higher in the present study. In the case of the reported mean R  
428 values in the cited study, we may compare it to the R values in Table 4 for all stations together at

429 daily time scale, that shows R values of 0.95 and 0.94 for ERA5 and MERRA-2 respectively,  
430 much lower than the ones reported in the cited research. The cited and present study agree  
431 reporting a moist bias for IWV from ERA5 and MERRA-2 respect to IWV<sub>GPS</sub> and IWV<sub>sp</sub>.

432 The dependence of the hourly  $\Delta$ IWV<sub>ERA5</sub> and  $\Delta$ IWV<sub>MERRA-2</sub> values on IWV<sub>sp</sub> and SZA is  
433 very low for IWV<sub>sp</sub> and negligible for SZA considering the magnitudes of R shown in figure 4.  
434 In the case of the dependence on SZA, this result agrees with the reported negligible effect of the  
435 SZA on the  $\Delta$ IWV<sub>sp</sub> - Sonde in Antuña-Marrero et al., (2022).

#### 436 **4 Conclusions**

437 The present study reports the first comparison specific to the Arctic thus far between  
438 IWV<sub>sp</sub> and IWV from ERA5 and MERRA-2 reanalyses. The IWV from both reanalyses show a  
439 predominant moist bias with respect to IWV<sub>sp</sub>. At the individual stations the daily mean IWV  
440 from reanalyses increases in accuracy and correlation but decreases in the precision with respect  
441 to the hourly values. Also, at station level and both at hourly and daily scales, the IWV<sub>ERA5</sub>  
442 values match better the observed IWV<sub>sp</sub> than the IWV<sub>MERRA-2</sub>. That pattern is also present at the  
443 sub-regional scale. The correlations between the hourly reanalyses' differences with IWV<sub>sp</sub>  
444 show a very low dependence on IWV<sub>sp</sub> values and no dependence at all on SZA, which points at  
445 both reanalyses as the main sources of the  $\Delta$ IWV<sub>ERA5</sub> and  $\Delta$ IWV<sub>MERRA-2</sub>. The set of IWV<sub>sp</sub> for  
446 AERONET in the Arctic could be used as a secondary standard in the Arctic, with the potential  
447 to conduct validations of other sources of IWV information with a primary standard dataset like  
448 the IWV from radiosonde observations.

#### 449 **Acknowledgments**

450 The authors are grateful to the Spanish Ministry of Science, Innovation and Universities  
451 for the support through the TRIPOLI project (PID2021-127588OB-I00) and to the Junta de  
452 Castilla y León AEROCYL project (VA227P20). This publication is part of the TED2021-  
453 131211B-I00 project funded by MCIN/AEI/10.13039/501100011033 and European Union  
454 “NextGenerationEU”/PRTR. J.C. Antuña-Marrero has been partially supported by the European  
455 Metrology Program for Innovation and Research (EMPIR) within the joint research project  
456 EMPIR 19ENV04 MAPP. The EMPIR is jointly funded by the EMPIR participating countries  
457 within EURAMET and the European Union. Thanks are due to AERONET-PHOTONS- RIMA  
458 staff for providing observations and for the maintenance of the networks. We also thank the PI  
459 and staff from the AERONET sites used in this study. ERA5 data (ECWMF, 2023) was  
460 downloaded from the Copernicus Climate Change Service. MERRA-2 data, GMAO (2023), was  
461 downloaded from the NASA Global Modeling and Assimilation Office (GMAO) (2023).

#### 462 **Conflict of Interest**

463 The authors declare no conflicts of interest relevant to this study.

#### 464 **Data Availability Statement**

465 The MERRA-2 reanalysis data are obtained from National Aeronautics and Space  
466 Administration, Global Modeling and Assimilation Office (GMAO, 2023), available at

467 [https://disc.gsfc.nasa.gov/datasets/M2I1NXINT\\_5.12.4/summary](https://disc.gsfc.nasa.gov/datasets/M2I1NXINT_5.12.4/summary). The ERA5 reanalysis data are  
468 obtained from European Centre for Medium-Range Weather Forecasts (ECMWF, 2023),  
469 available at <https://doi.org/10.24381/cds.adbb2d47>. AERONET sun photometer data are obtained  
470 from AErosol RObotic NETwork (AERONET, 2023) available at  
471 [https://aeronet.gsfc.nasa.gov/new\\_web/data.html](https://aeronet.gsfc.nasa.gov/new_web/data.html).

472 **References**

473 AERONET, (2023), Integrated water vapor [Dataset]. AErosol RObotic NETwork,  
474 [https://aeronet.gsfc.nasa.gov/new\\_web/index.html](https://aeronet.gsfc.nasa.gov/new_web/index.html)

475 Alraddawi, D., Sarkissian, A., Keckhut, P., Bock, O., Noël, S., Bekki, S., Irbah, A., Meftah, M.,  
476 and Claud, C., (2018), Comparison of total water vapour content in the Arctic derived from GNSS,  
477 AIRS, MODIS and SCIAMACHY, Atmos. Meas. Tech., 11, 2949–2965,  
478 <https://doi.org/10.5194/amt-11-2949-2018>

479 Antuña-Marrero, J. C., Román, R., Cachorro, V. E., Mateos, D., Toledano, C., Calle, A., Antuña-  
480 Sánchez, J. C., Vaquero-Martínez, J., Antón, M., de Frutos Baraja, Á. M., (2022), Integrated water  
481 vapor over the Arctic: Comparison between radiosondes and sun photometer observations,  
482 Atmospheric Research, 270,106059, <https://doi.org/10.1016/j.atmosres.2022.106059>

483 Box, J.E., Colgan, W., Christensen, T., Schmidt, N., Lund, M., Parmentier, F., Ross Brown, U.,  
484 Bhatt, E., Euskirchen, V., Romanovsky, J., Walsh, J. Overland, Muyin Wang, R., Corell, W.,  
485 Meier, B., Wouters, S., Mernild, J., Mård, J., Pawlak, M.S., (2019), Key indicators of Arctic  
486 climate change 1971–2017. Environ. Res. Lett. 14, 045010.  
487 <https://iopscience.iop.org/article/10.1088/1748-9326/aafc1b/meta>

488 Crewell, S., Eboll, K., Konjari, P., Mech, M., Nomokonova, T., Radovan, A., Strack, D., Triana-  
489 Gómez, A. M., Noël, S., Scarlat, R., Spreen, G., Maturilli, M., Rinke, A., Gorodetskaya, I., Viceto,  
490 C., August, T., and Schröder, M., (2021), A systematic assessment of water vapor products in the

491 Arctic: from instantaneous measurements to monthly means, *Atmos. Meas. Tech.*, 14, 4829–4856,  
492 <https://doi.org/10.5194/amt-14-4829-2021>

493 Dufour, A., Zolina, O., & Gulev, S. K., (2016), Atmospheric Moisture Transport to the Arctic:  
494 Assessment of Reanalyses and Analysis of Transport Components, *Journal of Climate*, 29(14),  
495 5061-5081. <https://journals.ametsoc.org/view/journals/clim/29/14/jcli-d-15-0559.1.xml>

496 ECMWF, (2016), IFS Documentation CY41R2 - Part I: Observations, 72 pp.,  
497 <https://www.ecmwf.int/en/elibrary/79695-ifs-documentation-cy41r2-part-i-observations>

498 ECMWF, (2023), Total column water vapour [Dataset]. ERA5 hourly data on pressure levels from  
499 1940 to present. <https://doi.org/10.24381/cds.adbb2d47>

500 Gelaro, R., McCarty, W., Suárez, et al., (2017), The Modern-Era Retrospective Analysis for  
501 Research and Applications, Version 2 (MERRA-2), *Journal of Climate*, 30(14), 5419-5454.  
502 Retrieved Jun 16, (2022), from <https://doi.org/10.1175/JCLI-D-16-0758.1>

503 Giles, D. M., Sinyuk, A., Sorokin, M. G., Schafer, J. S., Smirnov, A., Slutsker, I., Eck, T. F.,  
504 Holben, B. N., Lewis, J. R., Campbell, J. R., Welton, E. J., Korkin, S. V., and Lyapustin, A. I.,  
505 (2019), Advancements in the Aerosol Robotic Network (AERONET) Version 3 database –  
506 automated near-real-time quality control algorithm with improved cloud screening for Sun  
507 photometer aerosol optical depth (AOD) measurements, *Atmos. Meas. Tech.*, 12, 169–209,  
508 <https://doi.org/10.5194/amt-12-169-2019>

509 GMAO, (2023), MERRA-2\_inst1\_2d\_int\_Nx: 2d, 1-Hourly, Instantaneous, Single-Level,  
510 Assimilation, Vertically Integrated Diagnostics V5.12.4 [Dataset]. Goddard Space Flight Center  
511 Distributed Active Archive Center (GSFC DAAC), Accessed (16-FEB-2022)  
512 [https://disc.gsfc.nasa.gov/datasets/M2I1NXINT\\_5.12.4/summary](https://disc.gsfc.nasa.gov/datasets/M2I1NXINT_5.12.4/summary)

513 Graham, R. M., Hudson, S. R., & Maturilli, M. (2019). Improved performance of ERA5 in Arctic  
514 gateway relative to four global atmospheric reanalyses. *Geophysical Research Letters*, 46, 6138–  
515 6147. <https://doi.org/10.1029/2019GL082781>

516 Hersbach, H, Bell, B, Berrisford, P, et al., (2020), The ERA5 global reanalyses. *Q J R Meteorol  
517 Soc.*, 146: 1999– 2049. <https://doi.org/10.1002/qj.3803>

518 Holben, B. N., Eck, T. F., Slutsker, I., Tanre, D., Buis, J. P., Setzer, A., Vermote, E., Reagan, J.  
519 A., Kaufman, Y., Nakajima, T., Lavenue, F., Jankowiak, I., and Smirnov, A., (1998), AERONET  
520 – A federated instrument network and data archive for aerosol characterization, *Remote Sens.  
521 Environ.*, 66, 1–16, [https://doi.org/10.1016/S0034-4257\(98\)00031-5](https://doi.org/10.1016/S0034-4257(98)00031-5)

522 Huang, L., Mo, Z., Liu, L., Zeng, Z., Chen, J., Xiong, S., & He, H. (2021). Evaluation of hourly  
523 PWV products derived from ERA5 and MERRA-2 over the Tibetan Plateau using ground based  
524 GNSS observations by two enhanced models. *Earth and Space Science*, 8, e2020EA001516.  
525 <https://doi.org/10.1029/2020EA001516>

526 Leckner, B., (1978), The spectral distribution of solar radiation at the Earth's surface—Elements  
527 of a model. *Solar Energy*, 20(2), 143–150. [https://doi.org/10.1016/0038-092X\(78\)90187-1](https://doi.org/10.1016/0038-092X(78)90187-1)

528 Mauritzen, C., Rudels, B., Toole, J., 2013. The Arctic and Subarctic Oceans/Seas. *International  
529 Geophysics Ocean Circulation and Climate - A 21st Century Perspective*, pp. 443–470.  
530 <https://doi.org/10.1016/B978-0-12-391851-2.00017-9>

531 McCarty, W., L. Coy, R. Gelaro, A. Huang, D. Merkova, E. B. Smith, M. Sienkiewicz, and K.  
532 Wargan, (2016), MERRA-2 input observations: Summary and initial assessment. *Technical  
533 Report Series on Global Modeling and Data Assimilation*, Vol. 46, NASA Tech. Rep. NASA/TM–  
534 2016–104606, 61 pp. [Available online at <https://gmao.gsfc.nasa.gov/pubs/docs/McCarty885.pdf>]

535 Parker, W. S., (2016), Reanalyses and observations: What's the difference? *Bull. Amer. Meteor. Soc.*, 97, 1565–1572, <https://doi.org/10.1175/BAMS-D-14-00226.1>

537 Pérez-Ramírez, D., Whiteman, D.N., Smirnov, A., Lyamani, H., Holben, B.N., Pinker, R.,  
538 Andrade, M., Alados-Arboledas, L., (2014), Evaluation of AERONET precipitable water vapor  
539 versus microwave radiometry, GPS, and radiosondes at ARM sites. *J. Geophys. Res. Atmos.* 119,  
540 9596–9613. <https://doi.org/10.1002/2014JD021730>

541 Schröder, M., Lockhoff, M., Forsythe, J. M., Cronk, H. Q., Vonder Haar, T. H., & Bennartz, R.,  
542 (2016), The GEWEX Water Vapor Assessment: Results from Intercomparison, Trend, and  
543 Homogeneity Analysis of Total Column Water Vapor, *Journal of Applied Meteorology and*  
544 *Climatology*, 55(7), 1633-1649, <https://doi.org/10.1175/JAMC-D-15-0304.1>

545 Schröder, M.; Lockhoff, M.; Shi, L.; August, T.; Bennartz, R.; Borbas, E.; Brogniez, H.; Calbet,  
546 X.; Crewell, S.; Eikenberg, S.; et al.(2017), GEWEXWater Vapor Assessment (G-VAP); WCRP  
547 Report 16/2017;World Climate Research Programme (WCRP): Geneva, Switzerland, (2017);  
548 216p, Available online: <https://www.wcrp-climate.org/resources/wcrp-publications> (accessed on  
549 15 January 2022).

550 Schröder, M., Lockhoff, M., Fell, F., Forsythe, J., Trent, T., Bennartz, R., Borbas, E., Bosilovich,  
551 M. G., Castelli, E., Hersbach, H., Kachi, M., Kobayashi, S., Kursinski, E. R., Loyola, D., Mears,  
552 C., Preusker, R., Rossow, W. B., and Saha, S., (2018), The GEWEX Water Vapor Assessment  
553 archive of water vapour products from satellite observations and reanalyses, *Earth Syst. Sci. Data*,  
554 10, 1093–1117, <https://doi.org/10.5194/essd-10-1093-2018>

555 Schröder, M.; Lockhoff, M.; Shi, L.; August, T.; Bennartz, R.; Brogniez, H.; Calbet, X.; Fell, F.;  
556 Forsythe, J.; Gambacorta, A.; Ho, S.-p.; Kursinski, E.R.; Reale, A.; Trent, T.; Yang, Q., (2019),

557 The GEWEX Water Vapor Assessment: Overview and Introduction to Results and  
558 Recommendations. *Remote Sens.* 11, 251. <https://doi.org/10.3390/rs11030251>

559 Thorne, P. W., and R. S. Vose, (2010), Reanalyses suitable for characterizing long-term trends.  
560 *Bull. Amer. Meteor. Soc.*, 91, 353–362, <https://doi.org/10.1175/2009BAMS2858.1>

561 Vaquero-Martínez J, Antón M., (2021), Review on the Role of GNSS Meteorology in Monitoring  
562 Water Vapor for Atmospheric Physics. *Remote Sensing*; 13(12):2287,  
563 <https://doi.org/10.3390/rs13122287>

564 Vihma, T., J. Screen, M. Tjernström, B. Newton, X. Zhang, V. Popova, C. Deser, M. Holland, and  
565 T. Prowse, (2016), The atmospheric role in the Arctic water cycle: A review on processes, past and  
566 future changes, and their impacts, *J. Geophys. Res. Biogeosci.*, 121, 586–620,  
567 <https://doi.org/10.1002/2015JG003132>

568 Zhu, D.; Zhang, K.; Yang, L.; Wu, S.; Li, L. Evaluation and Calibration of MODIS Near-Infrared  
569 Precipitable Water Vapor over China Using GNSS Observations and ERA-5 Reanalysis Dataset.  
570 *Remote Sens.*, 13, 2761, 2021, <https://doi.org/10.3390/rs13142761>

571 Wang, Y., Yang, K., Pan, Z., Qin, J., Chen, D., Lin, C., et al., (2017), Evaluation of precipitable  
572 water vapor from four satellite products and four reanalyses datasets against GPS measurements  
573 on the southern Tibetan Plateau. *Journal of Climate*, 30(15), 5699–5713.  
574 <https://doi.org/10.1175/JCLI-D-16-0630.1>

575 Wang, S.; Xu, T.; Nie, W.; Jiang, C.; Yang, Y.; Fang, Z.; Li, M.; Zhang, Z. Evaluation of  
576 Precipitable Water Vapor from Five Reanalysis Products with Ground-Based GNSS Observations.  
577 *Remote Sens.* 12, 1817. <https://doi.org/10.3390/rs12111817>, 2020.

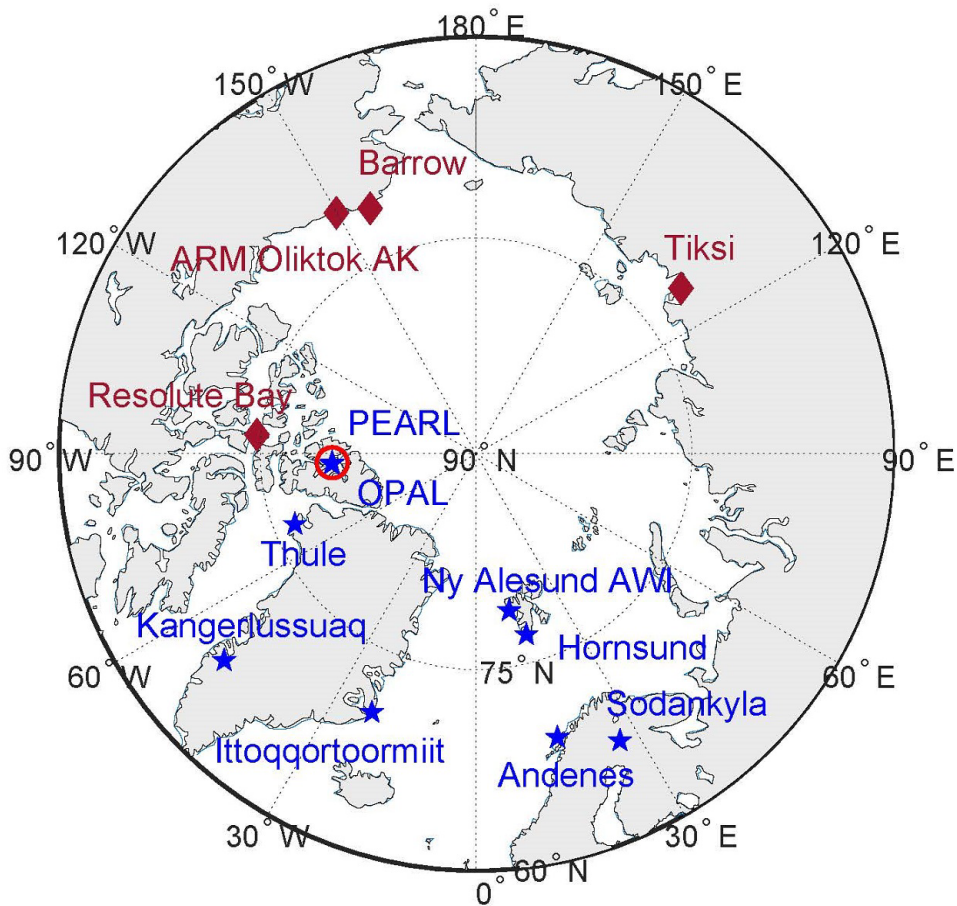
578 WMO, Guide to Instruments and Methods of Observation 558, 2021 - Measurement of  
579 Meteorological Variables, WMO-No. 8, 2021 edition, ISBN 978-92-63-10008-5, pp. 558, 2021.

580 Yuan, P., Van Malderen, R., Yin, X., Vogelmann, H., Awange, J., Heck, B., and Kutterer, H.,  
581 (2023), Characterizations of Europe's integrated water vapor and assessments of atmospheric  
582 reanalyses using more than two decades of ground-based GPS, *Atmos. Chem. Phys.*, 23, 3517–  
583 3541, <https://doi.org/10.5194/acp-23-3517-2023>

584

585 **Figures:**

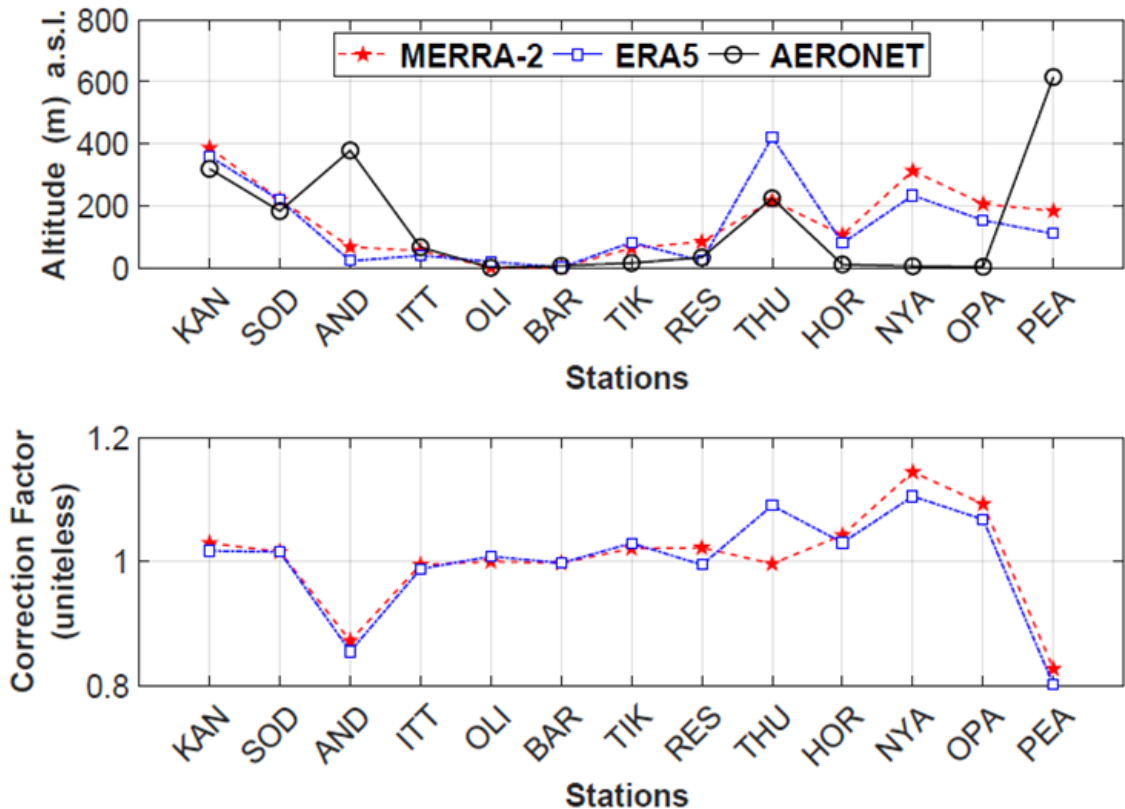
586



587

588 Figure 1: Map of the 13 Arctic AERONET stations used in the present study. Stations belonging to the GEA region  
589 are identified by blue stars and the ones in RACA region by brown diamonds, with their names following the same  
590 colors pattern. The blue star surrounded by a red circle represents the very close OPAL and PEARL stations in  
591 North Canada.

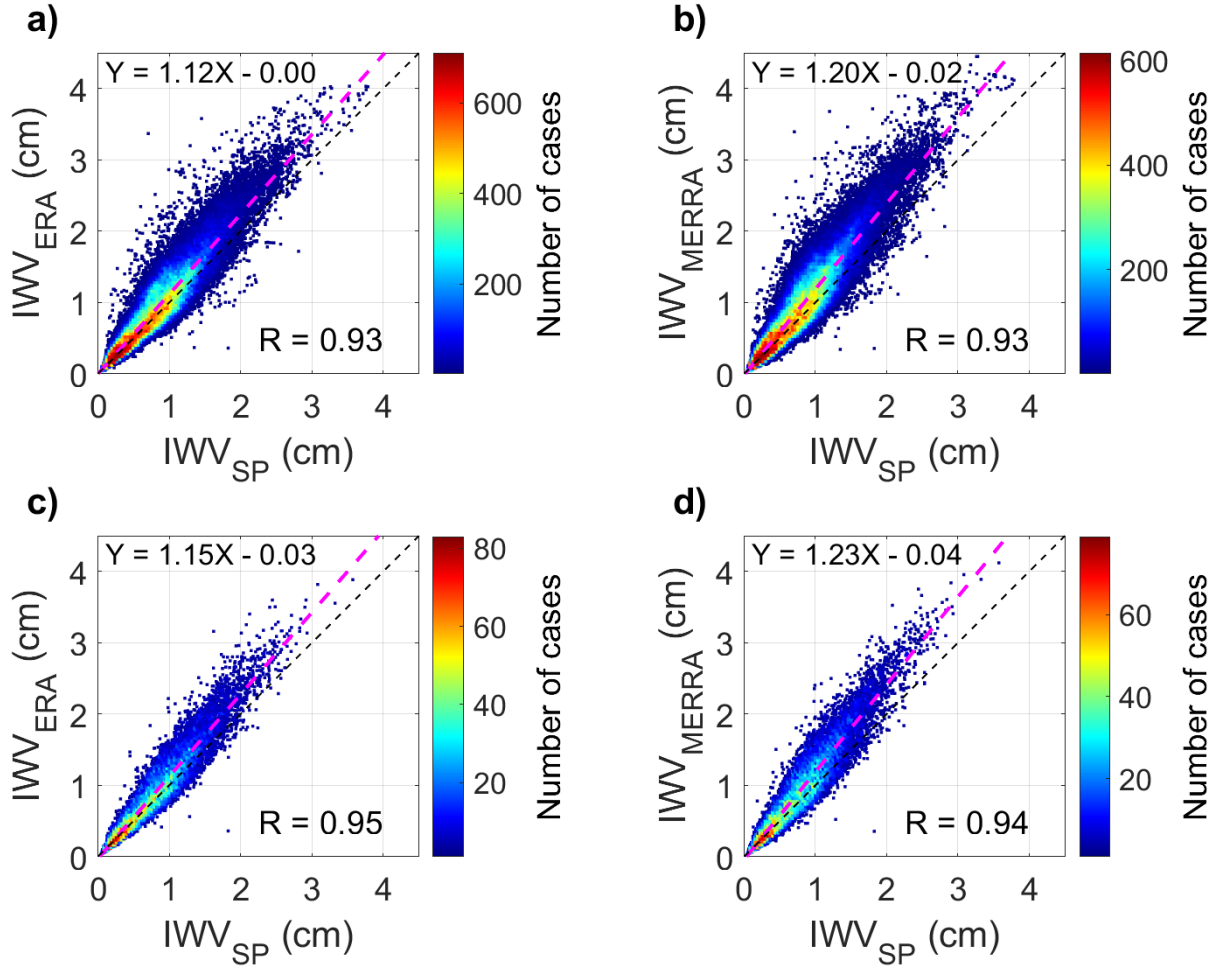
592



593

594 Figure 2: Top panel: altitudes of the 13 AERONET stations and the reanalyses respective altitudes.  
 595 Altitudes were bilinearly interpolated from the 4 grid points around the station. Bottom panel: IWV correction  
 596 factors applied to the IWV from ERA5 and MERRA-2 reanalyses. The stations abbreviations and names are: KAN  
 597 (Kangerlussuaq), SOD (Sodankyla), AND (Andenes), ITT (Ittoqqortoormiit), OLI (ARM Oliktok AK), BAR  
 598 (Barrow), TIK (Tiksi), RES (Resolute Bay), THU (Thule), HOR (Hornsund), NYA (Ny Ålesund AWI), OPA  
 599 (OPAL) and PEA (PEARL). For more information about the station see Table 1.

600

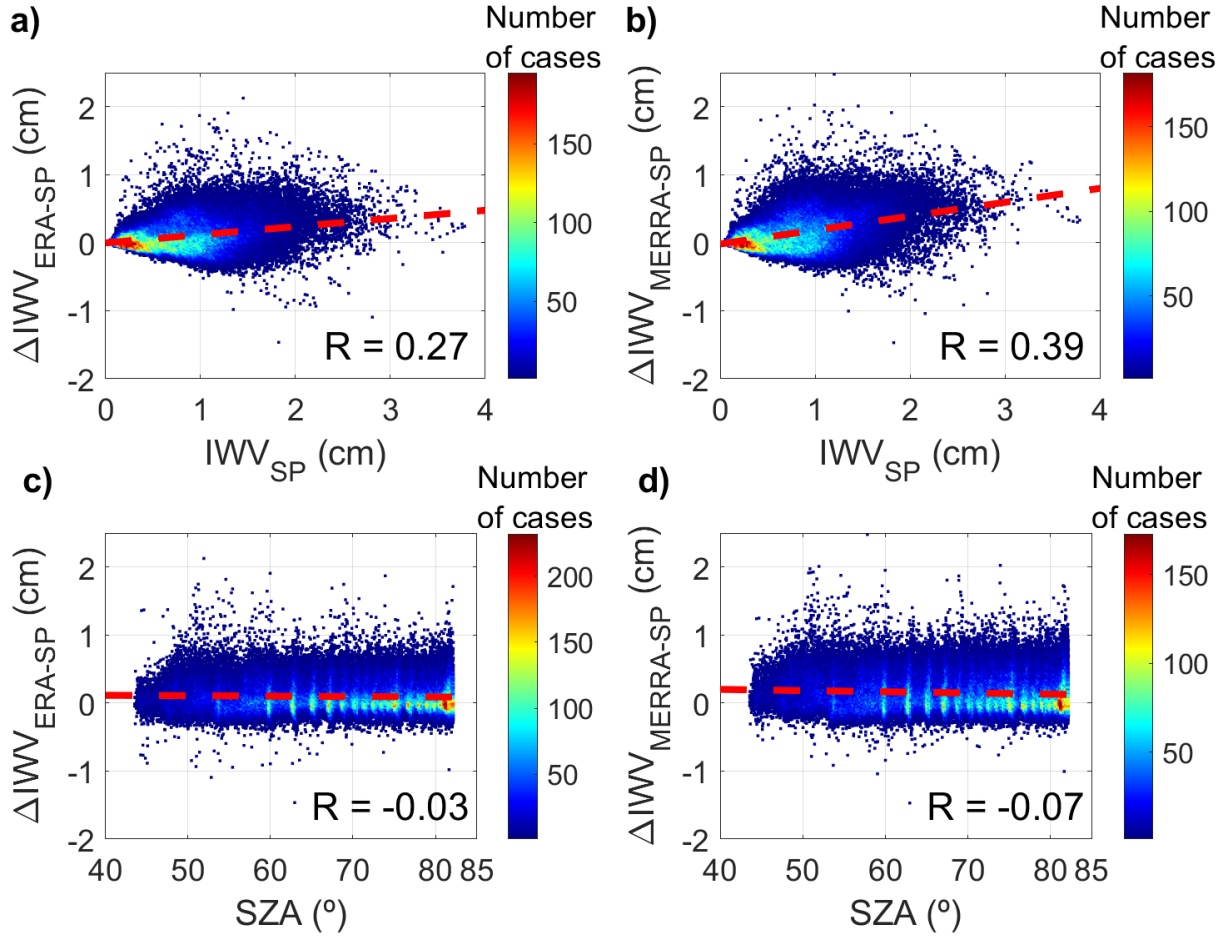


601

602

603      Figure 3: Density scatter plots of hourly and daily means for all the stations together for IWV<sub>ERA5</sub> &  
 604      IWV<sub>MERRA-2</sub>. Hourly values on top (panels a and b) and daily means in the bottom (panel c and d). ERA5 in the left  
 605      panels and MERRA-2 in the right panels. The magenta dashed lines denote the respective linear fits, and the black  
 606      dashed line denotes the 1:1 line.

607



608

609

610      Figure 4: In top panels, the scatter plots of the hourly for  $\Delta\text{IWV}_{\text{ERA5}}$  &  $\Delta\text{IWV}_{\text{MERRA-2}}$ . with respect to  
611       $\text{IWV}_{\text{SP}}$  (panels a and b respectively) for all the stations together. The red dashed lines denote the respective linear  
612      fits. Bottom panel also  $\Delta\text{IWV}_{\text{ERA5}}$  &  $\Delta\text{IWV}_{\text{MERRA-2}}$  scatter plots (panels c and d respectively) but with respect to the  
613      SZA.  
614  
615  
616

617 **Tables:**

618 Table 1: Information about all the available AERONET sun photometer stations in the Arctic,  
 619 listed in increasing latitude order. Geographical location and number of available instantaneous  
 620 observations, hourly and daily calculated values are given. Also, the beginning and ending dates  
 621 of the observations at each site. Stations having less than 1,500 hourly IWVsp values, shadowed  
 622 in gray, were discarded. The 13 numbered stations were used in the present study. The total  
 623 number of observations (last row), pertain only to the 13 stations used.

624

		AERONET station's location & altitude				Time coverage		# IWV available data		
No.	ID	Station	Lat	Long	H (m)	Begin	End	Obs.	Hourly	Daily
1	KAN	Kangerlussuaq	67.00	-50.62	320	01/04/2008	17/07/2020	55,636	11,056	1,386
2	SOD	Sodankyla	67.37	26.63	184	10/02/2007	19/06/2020	18,074	5,595	899
		Matorova FMI	68.00	24.24	340	10/09/2020	27/09/2021	7,535	482	77
		Abisko	68.35	18.82	390	27/04/2007	21/08/2007	1,091	373	61
		NEON TOOL	68.66	-149.37	843	12/02/2017	25/09/2021	7,094	1,136	280
3	AND	Andenes	69.28	16.01	379	04/06/2002	03/08/2020	39,681	8,609	1,244
4	ITT	Ittoqqortoormiit	70.48	-21.95	68	10/05/2010	27/09/2019	25,991	7,728	885
5	OLI	ARM Oliktok AK	70.50	-149.88	2	23/09/2013	19/06/2021	20,171	3,219	587
		NEON BARR	71.28	-156.62	6	19/04/2017	09/10/2021	1,523	472	107
6	BAR	Barrow	71.31	-156.66	8	30/07/1997	11/08/2020	30,553	7,946	1,261
7	TIK	Tiksi	71.59	128.92	17	08/06/2010	07/09/2015	4,634	1,786	335
8	RES	Resolute Bay	74.71	-94.97	35	04/07/2004	25/09/2019	73,529	7,064	866
9	THU	Thule	76.52	-68.77	225	15/03/2007	03/10/2021	65,615	13,864	1,582
10	HOR	Hornsund	77.00	15.54	12.4	07/05/2004	04/10/2020	18,951	6,562	1,024
		Longyearbyen	78.22	15.65	30	25/04/2003	13/08/2018	1,841	707	112
11	NYA	Ny Ålesund AWI	78.92	11.92	7	01/06/2017	19/05/2021	15,917	2,134	305
		Ny Ålesund	78.93	11.86	46	22/03/2006	01/04/2006	711	59	9
12	OPA	OPAL	79.99	-85.94	5	02/04/2007	13/06/2021	94,498	10,067	1,031
13	PEA	PEARL	80.05	-86.42	615	21/03/2007	06/09/2019	137,779	12,555	1,103
		North_Pole	88.80	24.25	1	18/04/2002	09/06/2002	309	97	17
		<b>Totals</b>						<b>601,029</b>	<b>98,185</b>	<b>12,158</b>

625

626 Table 2: Statistics of the comparison of hourly ERA & MERRA for each site for all the available  
 627 observations. The highest values of STD, rSTD, R and the absolute values of MBE and rMBE  
 628 among the 13 stations are highlighted in bold, and the lowest values in grayish background.

629

Station	IWV <sub>ERA</sub> vs IWV <sub>sp</sub>							IWV <sub>MERRA-2</sub> vs IWV <sub>sp</sub>						
	STD cm	rSTD/ %	MBE/ cm	rMBE/ %	Slope	Interc/ cm	R	STD /cm	rSTD/ %	MBE/ cm	rMBE/ %	Slope	Interc/ cm	R
<b>Kangerlussuaq</b>	0.12	14.9	0.01	0.6	0.95	0.04	0.96	0.14	16.7	0.06	6.90	1.02	0.04	0.95
<b>Sodankyla</b>	0.15	12.9	0.14	12.7	1.12	0.01	0.98	0.21	18.9	0.30	26.90	1.24	0.04	<b>0.98</b>
<b>Andenes</b>	0.16	16.3	0.25	25.3	1.18	0.08	0.98	0.19	19.7	0.35	35.90	1.25	0.11	0.97
<b>Ittoqqortoormiit</b>	0.09	11.0	-0.10	-11.7	0.89	-0.01	0.97	0.11	12.9	-0.02	-2.70	1.03	-0.05	0.96
<b>ARM_Oliktok_AK</b>	0.18	16.2	0.12	11.3	1.08	0.03	0.96	0.21	19.8	0.21	19.50	1.17	0.02	0.96
<b>Barrow</b>	<b>0.25</b>	24.6	<b>0.34</b>	33.6	1.29	0.05	0.96	<b>0.28</b>	28.1	<b>0.36</b>	36.50	1.33	0.03	0.96
Tiksi	0.19	15.4	0.09	7.3	1.09	-0.02	0.95	0.24	19.4	0.22	17.80	1.18	-0.01	0.95
<b>Resolute_Bay</b>	0.13	15.5	0.10	12.2	1.08	0.04	0.96	0.16	19.3	0.14	16.10	1.13	0.03	0.94
Thule	0.08	13.6	-0.09	-14.7	0.87	-0.01	0.97	0.09	14.1	-0.09	-15.40	0.89	-0.03	0.97
Hornsund	0.09	11.5	-0.02	-2.4	1.01	-0.03	0.98	0.10	13.0	-0.05	-6.90	0.95	-0.02	0.97
<b>Ny_Alesund_AWI</b>	0.10	13.1	0.06	8.0	1.10	-0.02	<b>0.99</b>	0.12	15.9	0.06	8.00	1.07	0.01	<b>0.98</b>
<b>OPAL</b>	0.11	12.7	0.07	7.5	1.09	-0.02	0.97	0.16	18.3	0.17	19.40	1.23	-0.03	0.96
<b>PEARL</b>	0.18	<b>29.7</b>	0.30	<b>50.9</b>	1.43	0.04	0.97	0.22	<b>37.4</b>	0.35	<b>60.30</b>	1.55	0.03	0.96

630

631

632 Table 3: Statistics of the comparison of daily mean ERA & MERRA for each site. Daily mean  
 633 values of IWV<sub>ERA</sub> & IWV<sub>MERRA</sub> calculated using only the hourly coincident observations with  
 634 IWV<sub>sp</sub>. The highest values of STD, rSTD, R and the absolute values of MBE and rMBE among  
 635 the 13 stations are highlighted in bold, and the lowest values in grayish background.

636

Station	IWV <sub>ERA</sub> vs IWV <sub>sp</sub>							IWV <sub>MERRA</sub> vs IWV <sub>sp</sub>						
	STD /cm	rSTD/ %	MBE /cm	rMBE/ %	Slope	Interc/ cm	R	STD /cm	rSTD/ %	MBE/ cm	rMBE/ %	Slope	Interc/ cm	R
<b>Kangerlussuaq</b>	0.10	12.1	0.00	0.4	0.97	0.03	0.98	0.12	14.5	0.05	5.8	1.02	0.03	0.97
<b>Sodankyla</b>	0.13	11.7	0.16	14.2	1.15	0.00	<b>0.99</b>	0.20	17.6	0.30	26.9	1.25	0.02	<b>0.99</b>
<b>Andenes</b>	0.15	15.3	0.25	26.2	1.21	0.05	0.98	0.18	18.4	0.35	36.0	1.27	0.08	0.98
<b>Ittoqqortoormiit</b>	0.08	9.5	-0.09	-10.6	0.91	-0.02	0.98	0.10	12.0	-0.01	-1.8	1.05	-0.06	0.97
<b>ARM_Oliktok_AK</b>	0.14	12.8	0.12	11.0	1.09	0.02	0.98	0.18	16.7	0.21	19.4	1.18	0.02	0.97
<b>Barrow</b>	<b>0.22</b>	22.1	<b>0.34</b>	33.4	1.31	0.02	0.98	<b>0.25</b>	25.2	<b>0.37</b>	36.6	1.36	0.01	0.97
Tiksi	0.14	11.9	0.09	7.3	1.11	-0.04	0.98	0.20	16.6	0.20	16.8	1.20	-0.04	0.97
<b>Resolute_Bay</b>	0.11	12.8	0.10	11.6	1.09	0.02	<b>0.97</b>	0.14	16.5	0.13	15.5	1.14	0.01	0.96
Thule	0.07	12.1	-0.09	-14.5	0.89	-0.02	0.98	0.08	12.6	-0.09	-15.0	0.91	-0.03	0.97
Hornsund	0.08	10.7	-0.01	-1.8	1.04	-0.04	0.98	0.09	11.0	-0.05	-6.6	0.97	-0.03	0.98
<b>Ny_Alesund_AWI</b>	0.09	10.6	0.07	8.8	1.11	-0.02	0.99	0.12	14.6	0.08	9.6	1.10	-0.01	0.98
<b>OPAL</b>	0.10	11.3	0.07	8.4	1.11	-0.02	0.98	0.15	16.9	0.17	19.7	1.24	-0.04	0.97
<b>PEARL</b>	0.18	<b>29.7</b>	0.30	<b>51.0</b>	1.49	0.02	0.98	0.22	<b>36.8</b>	0.35	<b>59.5</b>	1.60	0.00	0.98

637

638

639

640 Table 4: Statistics of the comparison of hourly and daily mean ERA and MERRA for GEA and  
 641 RACA regions and for all the stations. Daily mean values of ERA and MERRA were calculated  
 642 using only the hourly observations coincident with IWVsp.

643

Region/ Scale	IWV <sub>ERA</sub> vs IWVsp							IWV <sub>MERRA</sub> vs IWVsp							N. Observ .
	STD/ cm	rSTD/ %	MBE/ cm	rMBE/ %	Slope	Interc/ cm	R	STD/ cm	rSTD /	MBE/ cm	rMBE/ %	Slope	Interc/ cm	R	
<b>GEA Hr</b>	0.19	24.4	0.07	8.9	1.08	0.01	0.93	0.24	30.0	0.13	16.0	1.18	-0.01	0.92	78,170
<b>GEA Dy</b>	0.18	22.3	0.07	8.8	1.11	-0.02	0.95	0.23	27.9	0.12	15.2	1.20	-0.04	0.93	9,207
<b>RACA Hr</b>	0.23	23.0	0.20	20.1	1.18	0.03	0.95	0.25	25.6	0.25	25.2	1.24	0.01	0.95	20,015
<b>RACA Dy</b>	0.21	20.9	0.20	20.1	1.19	0.01	0.96	0.23	23.2	0.25	25.4	1.26	-0.01	0.96	2,951
<b>ALL Hr</b>	0.21	24.9	0.10	11.6	1.12	0.00	0.93	0.24	29.5	0.15	18.2	1.20	-0.02	0.93	98,185
<b>ALL Dy</b>	0.20	22.9	0.10	12.0	1.15	-0.03	0.95	0.23	27.3	0.15	18.1	1.23	-0.04	0.94	12,158

644

645 Table 5: Correlation coefficients (R) from the linear fits of the hourly  $\Delta$ IWV<sub>ERA</sub> and  $\Delta$ IWV<sub>MERRA</sub>  
 646 with IWVsp and SZA for each of the stations. R values higher than 0.50 are shadowed in gray.  
 647 The scale identifiers are: Hr (Hourly) and Dy (Daily).

648

Station	IWVsp		SZA		Number Cases
	ERA	MERRA	ERA	MERRA	
<b>Kangerlussuaq</b>	-0.16	0.06	-0.02	-0.07	11056
<b>Sodankyla</b>	0.51	0.68	-0.12	-0.19	5595
<b>Andenes</b>	0.55	0.64	0.00	-0.08	8609
<b>Ittoqqortoormiit</b>	-0.43	0.10	0.17	0.11	7728
<b>ARM_Oliktok_AK</b>	0.26	0.45	-0.03	-0.08	3219
<b>Barrow</b>	0.63	0.64	-0.11	-0.14	7946
<b>Tiksi</b>	0.25	0.42	-0.03	-0.10	1786
<b>Resolute_Bay</b>	0.23	0.30	0.02	0.02	7064
<b>Thule</b>	-0.49	-0.42	0.17	0.20	13864
<b>Hornsund</b>	0.05	-0.19	0.12	0.11	6562
<b>Ny_Alesund_AWI</b>	0.49	0.28	0.01	0.05	2134
<b>OPAL</b>	0.32	0.54	-0.06	-0.08	10067
<b>PEARL</b>	0.76	0.77	-0.17	-0.16	12,555

649